Proceedings of the 42nd IEEE
Conference on Decision and Control
Maui, Hawaii USA, December 2003

Effects of Dither Shapes in Nonsmooth Feedback Systems: Experimental Results and Theoretical Insight

Luigi Iannelli
Dip. di Informatica e Sistemistica
Università di Napoli Federico II
Napoli, Italy
luiannel@unina.it

Karl Henrik Johansson
Signals, Sensors & Systems
Royal Institute of Technology
Stockholm, Sweden
kallej@s3.kth.se

Ulf T. Jönsson
Dept. of Mathematics
Royal Institute of Technology
Stockholm, Sweden
ulfj@math.kth.se

Francesco Vasca
Dip. di Ingegneria
Università del Sannio
Benevento, Italy
vasca@unisannio.it

***Abstract*— Dither signals are commonly used to compensate for nonlinearities in feedback systems in electronics and mechanics. Recently, theoretical results were proposed for the analysis of a particularly interesting class of nonsmooth systems, namely relay feedback systems with triangular dither. In this paper the class of dither signals is enlarged by considering square and trapezoidal dither: it is shown how the dither shape affects the behavior of nonsmooth feedback systems, differently from the case of dither in Lipschitz continuous systems. Experimental results support this fact and a theoretical insight is given in order to explain the phenomena.**

I. Introduction

High-frequency dither signals are commonly used to compensate for nonlinearities in feedback control systems. The idea is that by injecting a suitably chosen high-frequency signal in the control loop, the nonlinear sector is effectively narrowed and the system can thereby be stabilized. A wide range of examples are found in the areas of electronics [1], [2], [3] and mechanics [4], [5]. Dithered systems in the past have been analyzed by using the describing function approach [6], [7]. Some other approaches exist in the literature. For example systems with smooth nonlinearity and smooth dither signal can be analyzed using powerful methods introduced in [8], [9], [10]. The smoothness assumptions are however often violated in practice [11]; for example, by nonsmooth static components such as switches and relays or by triangular and square wave dither signals. For classes of nonsmooth systems with high-frequency excitation, rigorous averaging analysis exists [1], [12].

Recently, new dither design methods based on averaging analysis were proposed for relay feedback systems with triangular dither [13]. Some other techniques for improving these results by exploiting a stability condition based on an LMI have been proposed in [14], [15]. In these papers we indicated through simulations that the considered averaging analysis carried out for triangular dither does not extend to square dither signals. In the current paper we present experimental evidence for this fact. We also give a geometric explanation. The behavior of a dithered relay feedback system is thus highly affected by the shape of the dither signal. This is in stark contrast to systems with Lipschitz continuous dynamics for which it can be shown that the form of the dither signal is not critical at all [8], [9]. The presented dynamical phenomena add to the behaviors known to appear in (autonomous) relay feedback systems, such as quasi-periodic orbits [16], chattering and sliding periodic orbits [17], [18], and asymmetric orbits [19].

The outline of the paper is as follows. Some notation is given in Section II. Section III presents experimental results for a DC motor application. The amplitude distribution function is introduced in Section IV. Section V is used to explain the influence of the dither shapes in the experiments.

The work by L. Iannelli and F. Vasca was supported by EC within the SICONOS project. The work by K. H. Johansson and U. Jönsson was supported the Swedish Research Council and by EC within the RECSYS project.

II. Preliminaries

Let us consider a relay nonlinearity

$$n(z) = \operatorname{sgn}(z) \triangleq \begin{cases} 1, & z > 0 \\ 0, & z = 0 \\ -1, & z < 0. \end{cases}$$

Suppose that a (deterministic) dither signal δ of period p is added to the input of the relay. The time averaging of the output y over a period p when the input z is constant is equal to

$$N(z) = \frac{1}{p}\int_0^p \operatorname{sgn}(z+\delta(t))\mathrm{d}t. \qquad (1)$$

This function is called the smoothed (or the averaged) nonlinearity and obviously depends on the shape of δ. Typical dither signals are triangular, sawtooth, sinusoidal, square wave and trapezoidal. The dithered relay feedback system is defined as

$$\dot{x}(t) = Lx(t) + bn(r + cx(t) + \delta(t)), \qquad x(0) = x_0. \qquad (2)$$

Here L, b, and c are constant matrices of dimensions $q \times q$, $q \times 1$, and $1 \times q$, respectively. The external reference r is constant. The smoothed system is given by

$$\dot{w}(t) = Lw(t) + bN(r + cw(t)), \qquad w(0) = w_0. \qquad (3)$$

In many cases the behavior of the dithered relay feedback system can be analysed by considering the corresponding smoothed system. In fact, it has been shown that with triangular and sawtooth dithers, the approximation error between the dithered and the smoothed system is proportional to the dither period and thus it can be made arbitrarily small by increasing the dither frequency [13].

For dither signals that have zero-slope over non-vanishing intervals (such as square wave dither), it has been shown that the smoothed system can behave significantly different from the dithered system [14]. In this paper we will illustrate these

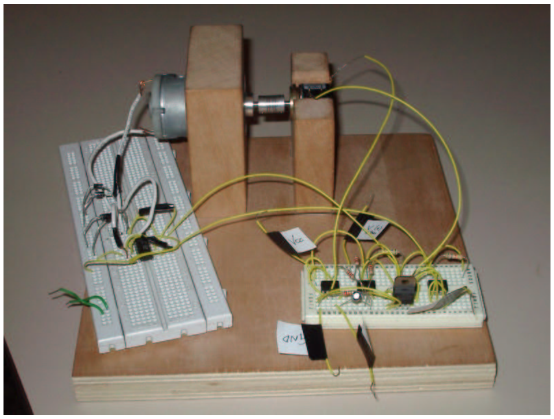

Fig. 1. Experimental setup of the DC motor position control system.

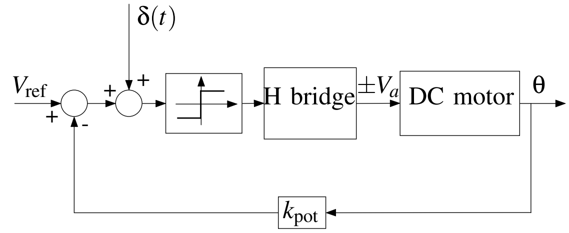

Fig. 2. Block diagram of the motor position control system.

phenomena by new experimental results followed by a theoretical explanation that the authors have recently rigorously proved and generalised to a wider class of nonlinear systems in [20].

III. Experimental Results

The experimental set-up showing the DC motor control system is reported in Fig. 1. Fig. 2 shows the corresponding block scheme. The control objective is to put the motor shaft at a desired angular position. The DC motor is modeled as an electric (armature) circuit subsystem with a given armature resistance R_a and inductance L_a, and a mechanical subsystem with inertia J and viscous coefficient β. The motor provides a torque proportional to the armature current i_a through the torque constant k_t and a counter electromagnetic force proportional to the rotor speed through the constant k_e. The angular position of the shaft θ is measured by using a rotational potentiometer whose gain is k_{pot}. The motor supply voltage is $\pm V_a$ and is obtained through a full bridge DC/DC converter (H-bridge). This power amplifier has a logic input that selects a positive or negative supply voltage to the DC motor. The control loop is closed by comparing the position error $V_{\text{ref}} - k_{\text{pot}}\theta$ with a sawtooth waveform (the dither signal). The output of the relay is the input of the H-bridge driver. By introducing the state vector $x = \begin{pmatrix}\theta & \omega & i_a\end{pmatrix}^T$ we have

$$\dot{x}(t) = \begin{pmatrix} 0 & 1 & 0 \\ 0 & -\frac{\beta}{J} & \frac{k_t}{J} \\ 0 & -\frac{k_e}{L_a} & -\frac{R}{L_a} \end{pmatrix} x(t) \pm \begin{pmatrix} 0 \\ 0 \\ \frac{V_a}{L_a} \end{pmatrix}, \qquad (4)$$

where the signum depends on the output of the H-bridge. This control system corresponds to the dithered relay feedback system (2) with L and b as given in (4), and $c = \begin{pmatrix}-k_{\text{pot}} & 0 & 0\end{pmatrix}$. The external constant reference is equal to $r = V_{\text{ref}}$. The loop transfer function for the system is

$$-c(sI-L)^{-1}b = \frac{\frac{k_t k_{\text{pot}}}{J}\frac{V_a}{L_a}}{s\left[s^2 + s\left(\frac{\beta}{J} + \frac{R}{L}\right) + \frac{\beta R}{JL} + \frac{k_t k_e}{JL}\right]}. \qquad (5)$$

Let us consider a DC motor with the following parameters: $R = 2.510\,\Omega$, $L_a = 0.530\,\text{mH}$, $k_t = k_e = 5.700\,\text{mV}/(\text{rad}\cdot\text{s}^{-1})$, $\beta = 0.411\,\text{mN}\cdot\text{cm}/(\text{rad}\cdot\text{s}^{-1})$, $J = 31.400\,\text{g}\cdot\text{cm}^2$, $k_{\text{pot}} = 3/(2\pi)\,\text{V/rad}$. The motor supply voltage is set to $V_a = 2.500\,\text{V}$. Three dither shapes are considered: a sawtooth signal, a square wave signal, and a trapezoidal signal. The dither amplitude is in all cases equal to $A = 0.070$. With the parameters above, the loop transfer function is

$$-c(sI-L)^{-1}b = \frac{4.088\cdot 10^6}{s(s^2 + 4.737\cdot 10^3 s + 2.573\cdot 10^4)}. \qquad (6)$$

It can be shown (e.g., using the Popov criterion) that the smoothed systems corresponding to the sawtooth and trapezoidal dither cases are asymptotically stable, see [15]. For sawtooth dither, the approximation error between the dithered system and the smoothed system tends to zero as the dither frequency goes to infinity. Hence, since the smoothed system is asymptotically stable, the system output goes to zero as we increase the dither frequency. For trapezoidal dither, the assumptions of the averaging result in [15] are not fulfilled. In fact, the approximation error between the dithered system and the smoothed system may not tend to zero in this case, as was indicated by a theoretical example in [20]. In the following, we show that the DC motor application supports these conclusions: the system is stabilized with sawtooth dither, while it is not with trapezoidal or square wave dither.

Experiments were carried using sawtooth dither of frequencies 100, 200, and 500 Hz. Fig. 3 reports the angular position of the motor shaft under steady-state conditions. Note that by increased dither frequency the behavior of the dithered system converges to the behavior of the (stable) smoothed system (i.e., the system output converges to zero). The ratio between consecutive averages of the peak-to-peak values of the output signal is equal to 3.33 and 2.84 for 100–200 Hz and 200–500 Hz, respectively, which thus indicates the convergence rate. The averaging effect of the dither thus works properly in this case.

Fig. 4 shows experiments with trapezoidal dither. In this case, the system output shows a slow oscillation with a substantial amplitude for all three dither frequencies (note that the axes are not the same as in Fig. 3). The frequency of the oscillation is low compared to the dither frequency, and it seems to be relatively constant. In particular, note that by the increase of the dither frequency, the system output does not converge to zero, as was the case with sawtooth dither. Instead the ratio between consecutive averages of the peak-to-peak values of the output signal is equal to 1.97 and 0.86

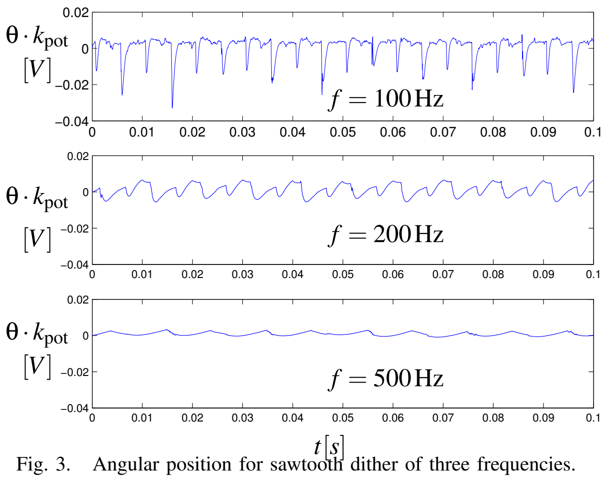

Fig. 3. Angular position for sawtooth dither of three frequencies.

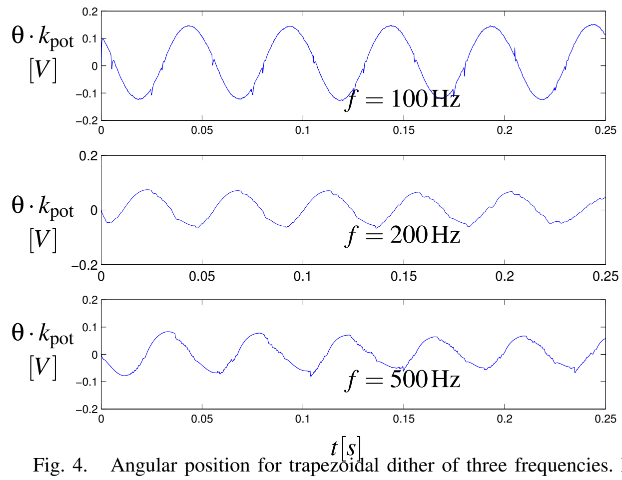

Fig. 4. Angular position for trapezoidal dither of three frequencies. Note the different scale compared to Fig. 3.

for 100–200 Hz and 200–500 Hz, respectively, so going from 200 to 500 Hz the amplitude of the oscillation is actually increasing.

A geometric illustration of these phenomena is obtained from phase diagrams. Fig. 5 shows a phase diagram for sawtooth dither, Figs. 6 and 7 show phase diagrams for trapezoidal dither, while Fig. 8 shows a phase diagram for square wave dither. The two hyperplanes highlighted in the figures are given by $\{x \in \mathbb{R}^3 : cx \pm A = 0\}$, where $A = 0.070$ is the amplitude of the dither. The hyperplanes bound the region in which the dither instantaneously can affect the input to the DC motor, since outside that region the sign of $cx + \delta$ is not affected by δ. In Fig. 5, where sawtooth dither was applied, we note that the trajectory is always far from the hyperplanes. In Figs. 6 and 7 it is shown that trapezoidal dither gives rise to trajectories that hit the hyperplanes. These periodic orbits show similarities to sliding and chattering orbits in autonomous relay feedback systems, which was recently thoroughly analyzed [17], [18], [19]. Note that even if the frequency was doubled in Fig. 7, the trajectory still intersects the hyperplanes. To investigate the limiting case of very high frequency, we applied square wave dither of 1 MHz. Fig. 8 shows the result. Although the trajectory does not intersect the hyperplanes in this case, the dither still does not stabilize the system about the origin.

IV. Amplitude Density Functions

To gain theoretical insight about the experimental results in the previous section we discuss the amplitude distribution function for the various dither signals. The amplitude distribution function $F_\delta(a)$ for a p-periodic dither signal δ is defined as the Lebesgue measure of the time intervals in which $\delta(t) \le a$ for $t \in [0, p)$, i.e.,

$$F_\delta(a) = \frac{1}{p}\mu\{t \in [0,p) : \delta(t) \le a\}. \tag{7}$$

A recent result [20] indicates that an important sufficient condition for the approximation error in the averaging analysis to tend to zero is that F_δ is absolutely continuous. Moreover, examples show that if F_δ is discontinuous, then the approximation error may not go to zero. We illustrate

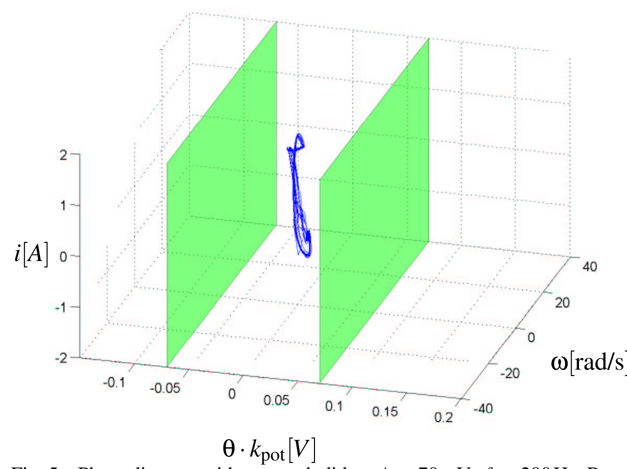

Fig. 5. Phase diagram with sawtooth dither, $A = 70$ mV, $f = 200$ Hz. Recall that the output signal is $\theta \cdot k_{pot}$, which has a small ripple as illustrated in Fig. 3.

next that this conclusion is confirmed also by the DC motor application.

By interpreting (1) as a Lebesgue-Stieltjes integral (e.g., [21]), it follows that for almost all z

$$\begin{aligned} N(z) &= \int_{\mathbb{R}} \operatorname{sgn}(z+a)\mathrm{d}F_\delta(a) \\ &= \int_{-z^+}^{\infty} \mathrm{d}F_\delta(a) - \int_{-\infty}^{-z^-} \mathrm{d}F_\delta(a) \\ &= 1 - F_\delta(-z^+) - F_\delta(-z^-). \end{aligned} \tag{8}$$

If $F_\delta(z)$ is continuous in $-z$ then $N(z) = 1 - 2F_\delta(-z)$, otherwise we have to take into account the left and right limits of F_δ in $-z$.

When the amplitude distribution function is absolutely continuous then the amplitude density function f_δ is well defined as the (Lebesgue integrable) solution to the equation

$$\mathrm{d}F_\delta = f_\delta(a)\mathrm{d}a, \tag{9}$$

In this case we have

$$N(z) = \int_{-\infty}^{\infty} \operatorname{sgn}(z+\delta) f_\delta(a)\mathrm{d}a.$$

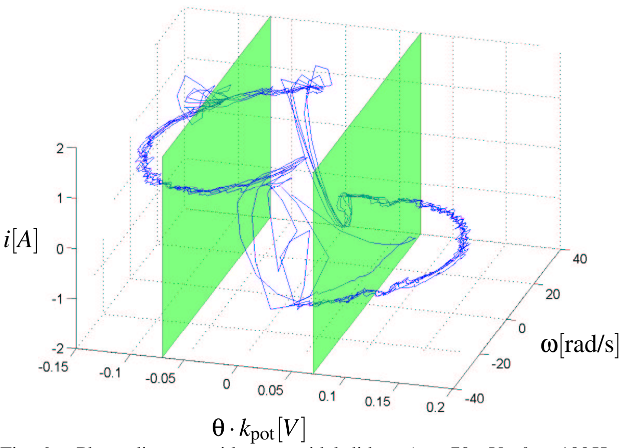

Fig. 6. Phase diagram with trapezoidal dither, $A = 70\,\text{mV}$, $f = 100\,\text{Hz}$.

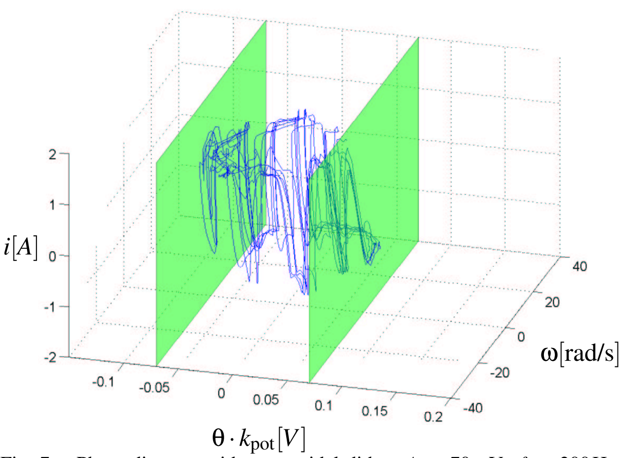

Fig. 7. Phase diagram with trapezoidal dither, $A = 70\,\text{mV}$, $f = 200\,\text{Hz}$.

If the amplitude distribution function has jump discontinuities we here represent these singularities with Dirac impulses in f_δ.

Note that a time average formula for deriving N was suggested in (1), while the analysis above suggest an output average formula. For the dither signals and nonlinearities in this paper, this two formulae are equal.

Let us discuss the amplitude density functions for the dithers applied to the DC motor. Fig. 9 shows the amplitude distribution function F_δ and the amplitude density function f_δ of triangular dither applied to the relay. The corresponding smoothed nonlinearity N is also reported. A sawtooth dither with amplitude A and period p has the same amplitude distribution function and thus also the same smoothed nonlinearity. Note that N has Lipschitz constant equal to $1/A < \infty$, while the original relay nonlinearity is discontinuous. The dither thus has "smoothed" the relay.

The amplitude distribution and density functions of square wave and trapezoidal dither and the corresponding smoothed nonlinearities are reported in Fig. 10 and Fig. 11. In these cases, the amplitude density functions have two Dirac impulses, which lead to that the smoothed nonlinearity is discontinuous (at $z = \pm A$). Thus for the square wave and trapezoidal dithers the smoothed nonlinearity has discontinuities,

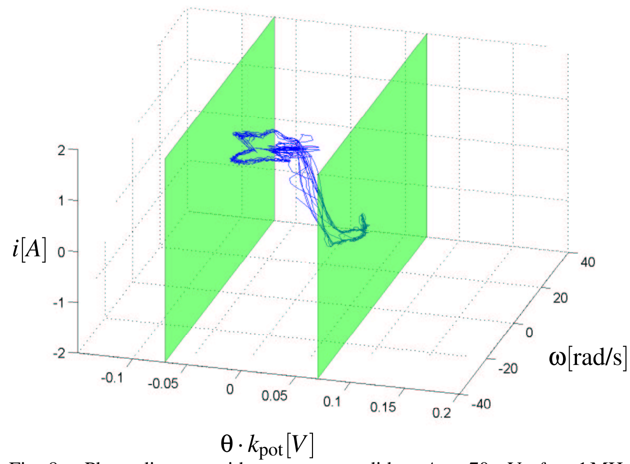

Fig. 8. Phase diagram with square wave dither, $A = 70\,\text{mV}$, $f = 1\,\text{MHz}$.

which is in contrast to the triangular case. The discontinuous system gives rise to oscillations, as shown in the previous section. It is easy to see that dither signals that are constant over non-vanishing time intervals has Dirac impulses in their amplitude density functions, and thus discontinuous smoothed nonlinearities. This class of of zero-slope dither signals show interesting dynamical behavior and has to be carefully analysed.

V. Conclusions

The paper points towards a need for a framework for analyzing dithered nonsmooth systems. Existing results mainly consider special cases, such as relay systems with triangular dither [13], [15], PWM converters with ramp comparison [1], and various other PWM systems [12]. For Lipschitz continuous systems, a nice theory was developed by Zames and Shneydor [8], [9], which covers a large class of dither signals. For discontinuous systems, however, the shape of the dither signal is important, as shown in this paper. The approximation error between the dithered and the smoothed systems converges to zero as the frequency of the dither tends to infinity, only under certain regularity assumptions. It was indicated in the paper that for discontinuous systems, an important assumption is that the amplitude distribution function should be absolutely continuous, i.e. no jump discontinuities are allowed. If this assumption does not hold, the approximation error may not go to zero. Recently this conjecture was theoretically justified through an averaging result for a quite general class of nonsmooth systems and periodic dither signals, see [20]. In particular the class of the considered dithered systems include the following nonsmooth feedback system:

$$\dot{x} = f_0(x,d) + f_1(x,d)n(g(x,d,r) + \delta), \qquad x(0) = x_0,$$

where f_0, f_1 and g are Lipschitz, the reference r and the disturbance d are Lipschitz signals and the nonlinearity n is assumed to be Borel-measurable and of bounded variation.

VI. Acknowledgements

The authors would like to thank Mr. Luca Piedimonte for his help in deriving simulations and experimental results.

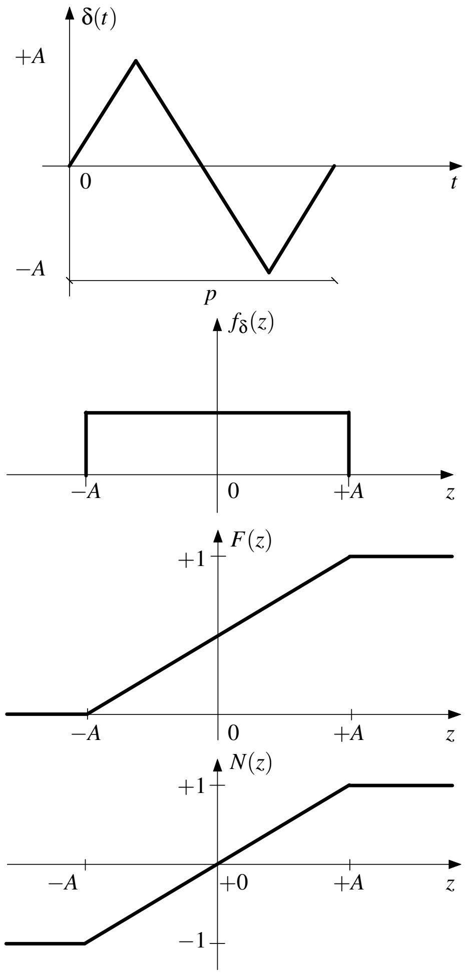

Fig. 9. Triangular dither signal, its amplitude density function, distribution function and the corresponding smoothed nonlinearity.

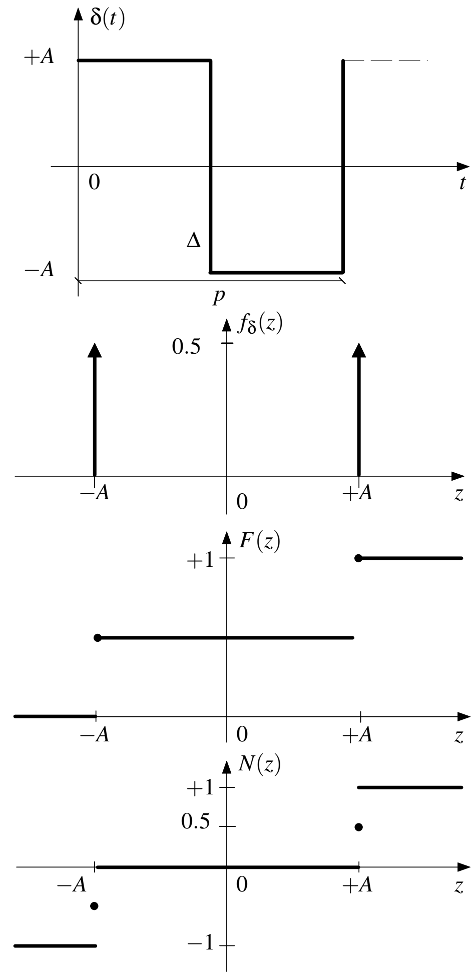

Fig. 10. Square wave dither signal, its amplitude density function, distribution function and the corresponding smoothed nonlinearity.

VII. REFERENCES

[1] B. Lehman and R. Bass, "Extensions of averaging theory for power electronics systems", *IEEE Transactions on Power Electronics*, vol. 11, no. 4, pp. 542–553, 1996.

[2] A. V. Peterchev and S. R. Sanders, "Quantization resolution and limit cycling in digitally controlled PWM converters", in *Proc. IEEE Power Electronics Specialists Conf.*, Vancouver, Canada, June 2001.

[3] R. M. Gray and D. L. Neuhoff, "Quantization", *IEEE Transactions on Information Theory*, vol. 44, no. 6, pp. 2325–2383, 1998.

[4] B. Armstrong-Helouvry, *Control of Machines with Friction*, Kluwer Academic Publisher, Boston, 1991.

[5] B. Armstrong-Helouvry, P. Dupont, and C. Canudas de Wit, "A survey of models, analysis tools and compensation methods for control of machines with friction", *Automatica*, vol. 30, no. 7, pp. 1083–1138, 1994.

[6] D. Atherton, *Nonlinear Control Engineering*, Van Nostrand Reinhold Co., London, 1975.

[7] A. Gelb and W. Vander-Velde, *Multiple Input Describing Functions*, McGraw-Hill, 1968.

[8] G. Zames and N. A. Shneydor, "Dither in non-linear systems", *IEEE Transactions on Automatic Control*, vol. 21, no. 5, pp. 660–667, October 1976.

[9] G. Zames and N. A. Shneydor, "Structural stabilization and quenching by dither in non-linear systems", *IEEE Transactions on Automatic Control*, vol. 22, no. 3, pp. 352–361, June 1977.

[10] S. Mossaheb, "Application of a method of averaging to the study of dither in non-linear systems", *International Journal of Control*, vol. 38, no. 3, pp. 557–576, September 1983.

[11] A. A. Pervozvanski and C. Canudas de Wit, "Asymptotic analysis of the dither effect in systems with friction", *Automatica*, vol. 38, no. 1, pp. 105–113, January 2002.

[12] A. Kh. Gelig and A. Churilov, *Stability and Oscillations of Nonlinear Pulse Modulated Systems*, Birkhäuser, Berlin, 1998.

[13] L. Iannelli, K.H. Johansson, U. Jönsson, and F. Vasca, "Analysis of dither in relay feedback systems", in

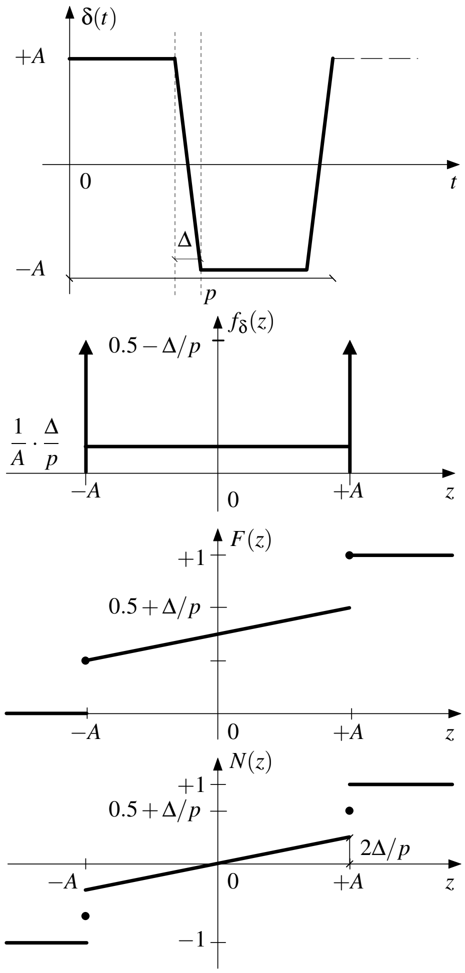

Fig. 11. Trapezoidal dither signal, its amplitude density function, distribution function and the corresponding smoothed nonlinearity.

Proc. of IEEE Conference on Decision and Control, Las Vegas, Nevada, USA, December 2002.

[14] L. Iannelli, K. H. Johansson, U. Jönsson, and F. Vasca, "Practical stability and limit cycles of dithered relay feedback systems", in *Proc. of IEE European Control Conference*, Cambridge, UK, September 2003.

[15] L. Iannelli, K. H. Johansson, U. Jönsson, and F. Vasca, "Dither for smoothing relay feedback systems: an averaging approach", *IEEE Transactions on Circuits and Systems, Part I*, vol. 50, no. 8, pp. 1025–1035, August 2003.

[16] P. A. Cook, "Simple feedback systems with chaotic behaviour", *Systems & Control Letters*, vol. 6, pp. 223–227, 1985.

[17] K. H. Johansson, A. Rantzer, and K. J. Åström, "Fast switches in relay feedback systems", *Automatica*, vol. 35, no. 4, pp. 539–552, April 1999.

[18] K. H. Johansson, A. Barabanov, and K. J. Åström, "Limit cycles with chattering in relay feedback systems", *IEEE Transactions on Automatic Control*, vol. 47, no. 9, 2002.

[19] M. di Bernardo, K. H. Johansson, and F. Vasca, "Self-oscillations and sliding in relay feedback systems: Symmetry and bifurcations", *International Journal of Bifurcations and Chaos*, vol. 11, no. 4, pp. 1121–1140, 2000.

[20] L. Iannelli, K.-H. Johansson, U. Jönsson, and F. Vasca, "Conditions on the dither shape in the averaging of switched systems", Tech. Rep. TRITA/MAT-03-OS08, Department of Mathematics, Royal Institute of Technology, September 2003.

[21] S.J. Taylor, *Introduction to Measure and Integration*, Cambridge University Press, 1966.